PNAS
www.pnas.org

Supplementary Information for

Fibroblasts lacking nuclear lamins do not have nuclear blebs or protrusions but nevertheless have frequent nuclear membrane ruptures

N.Y. Chen, P. Kim, T. Weston, L. Edillo, Y. Tu, L.G. Fong, and S.G. Young

Stephen G. Young, M.D.
Email: sgyoung@mednet.ucla.edu

This PDF file includes:

Supplementary Information Materials and Methods
Figs. S1 to S9
Tables S1 to S2
Captions for movies S1 to S15
References for SI reference citations

Other supplementary materials for this manuscript include the following:

Movies S1 to S15

www.pnas.org/cgi/doi/10.1073/pnas.1812622115

SI Materials and Methods

Cell Culture. To generate triple-knockout (TKO) MEFs (*Lmna*$^{-/-}$*Lmnb1*$^{-/-}$*Lmnb2*$^{-/-}$) and A1B0 MEFs (*Lmna*$^{+/-}$*Lmnb1*$^{-/-}$*Lmnb2*$^{-/-}$), *Lmna*$^{-/-}$*Lmnb1*$^{fl/fl}$ *Lmnb2*$^{fl/fl}$ and *Lmna*$^{+/-}$*Lmnb1*$^{fl/fl}$ *Lmnb2*$^{fl/fl}$ MEFs, respectively, were treated with *Cre* adenovirus (Gene Transfer Vector Core) three times at 1,000 MOI each. To generate B1KO MEFs (*Lmna*$^{+/+}$*Lmnb1*$^{-/-}$*Lmnb2*$^{+/+}$), E13.5 mouse embryos were harvested from *Lmnb1*$^{+/-}$ breeder pairs. Cultures of MEFs were grown in monolayer cultures at 37°C with 5–7% CO2 and maintained in DMEM (Gibco) containing 10% fetal bovine serum (FBS; Hyclone) and 100 units/ml of penicillin and 100 μg/ml of streptomycin.

Quantitative RT-PCR Studies. Total RNA was isolated and treated with DNase I (Ambion). RNA was reverse-transcribed with random primers, oligo(dT), and SuperScript III (Invitrogen). qPCR reactions were performed on a 7900 Fast Real-Time PCR system (Applied Biosystems) with SYBR Green PCR Master Mix (Bioline). Transcript levels were determined by the comparative cycle threshold method and normalized to levels of cyclophilin A. All primers used are listed in Table S1.

Western Blots. Proteins were size-fractionated on 4–12% gradient polyacrylamide Bis-Tris gels (Invitrogen) and transferred to a nitrocellulose membrane. Membranes were blocked with Odyssey Blocking solution (LI-COR Biosciences) for 1 h at RT and then incubated with primary antibodies at 4°C overnight. After washing the membranes with PBS containing 0.1% Tween-20, they were incubated with infrared dye (IR)–labeled secondary antibodies for 1 h at RT. The IR signals were quantified with an Odyssey infrared scanner (LI-COR Biosciences).

Immunofluorescence Microscopy and Image Analysis. For confocal immunofluorescence microscopy, images were obtained with a Zeiss LSM700 laser-scanning microscope with a Plan Apochromat 20×/0.80 objective (air) or a Plan Apochromat 100×/1.40 oil-immersion objective. Images along the *z*-axis were processed by Zen 2010 software (Zeiss). For live-cell imaging, image sequences were analyzed with ZEN (Zeiss) using only linear adjustments uniformly applied to the entire image region. For confocal image stacks, images were three-dimensionally reconstructed and displayed as maximum intensity projections. A nuclear rupture event was defined as NLS-GFP entry into the cytoplasm (in interphase cells only).

Nuclear Circularity. To quantify the variation in nuclear morphology, we computed nuclear circularity ($4\pi \times \text{area}/\text{perimeter}^2$) by measuring nuclear areas and perimeters of 100 cells for each genotype. The circularity measurement reaches a maximum value of 1.0 for a circle and decreases with shape irregularities (1).

Electron Microscopy. Cells were prepared for transmission electron microscopy (TEM) in two ways: 1) Embedding of non-adherent cells. Cell monolayers were fixed for 1 h in fixative solution containing 4% paraformaldehyde (EMS) and 2.5% glutaraldehyde (EMS) buffered with 0.1 M sodium cacodylate (Sigma) and then gently scraped from the dishes with a cell scraper (Corning). The suspension was centrifuged at 350 *g* for 15 min to generate a pellet. The pellets were allowed to fix for another 45 min before rinsing three times with 0.1 M sodium cacodylate and post-fixing with 1% osmium tetroxide (EMS) buffered with 0.1 M sodium cacodylate for 1 h at room temperature. Next, samples were rinsed three times with distilled water and stained overnight with 2% uranyl acetate (SPIChem) at 4˚C. Samples were rinsed three times with distilled water and dehydrated through a series of increasing acetone concentrations (30%, 50%, 70%, 85%, 95%, 100%; 3 × 10 min each) before infiltration with increasing concentrations of EMBed812 epoxy resin (EMS) in acetone (33% for 2 h; 66% overnight; 100% for 4 h). Next, samples were embedded in fresh resin and polymerized in a vacuum oven for 24 h at 65˚C. 2) *En face* embedding of adherent cells. Cells were grown on Thermanox (Ted Pella) coverslips. Cells on coverslips were rinsed once with fixative solution (2.5% glutaraldehyde in 0.1 M sodium cacodylate), and then fresh fixative was added for 1 h on ice. Next, cells were rinsed 5 × 2 min each with cold 0.1 M sodium cacodylate and then post-fixed with 2% osmium tetroxide in 0.1 M sodium cacodylate for 30 min on ice. Next, cells were rinsed 5 × 2 min with distilled water and stained overnight with 2% uranyl acetate at 4˚C. Cells were rinsed 5 × 2 min with distilled water and dehydrated through a series of increasing ethanol concentrations (30%, 50%, 70%, 85%, 95%, 100%; 3 × 2 min each) before being infiltrated with increasing

concentrations of EMBed812 epoxy resin in acetone (33% for 1 h; 66% overnight; 100% for 2 h). Next, coverslips were inverted onto a BEEM capsule filled to the top with fresh EMBed812 and polymerized in an oven at 65˚C for 48 h. Once polymerized, coverslips were peeled off of the block, leaving the monolayer of cells behind. For both methods, the polymerized blocks were removed from the tubes, were trimmed and 65-nm sections were generated with a Leica UC6 ultramicrotome and picked up on freshly glow-discharged copper grids (Ted Pella) that were coated with formvar and carbon. Sections were then stained with Reynold's lead citrate solution for 10 min. Images were acquired with an FEI T12 transmission electron microscope set to 120kV accelerating voltage using a Gatan 2kX2k digital camera.

Cell Stretching. Flexible polydimethylsiloxane (PDMS) membranes were prepared in 150-mm culture dishes with the Sylgard 184 silicone elastomer kit (Dow-Corning #3097358-1004). Membranes strips (7 × 0.8 cm) were activated with a plasma cleaning machine, treated with 2% 3-aminopropy-triethoxysilane at RT for 45 min, and then dried at 55° C for 30 min. The membranes were incubated with 0.5 mg/ml sulfo-SANPAH in HEPES buffer and crosslinked with UV exposure (300–460 nm) for 30 sec. The washed membranes were stored at 4° C in a 100 μg/ml collagen solution (PureCol 5005; Advanced Biomatrix). Cells (1×10^5) were added to individual membrane strips in molds and incubated in media for 24 h and then clamped into a custom-built stretching device. The brackets holding the membranes were attached to an L12 linear actuator (Actuonix) controlled by a multifunction DAQ device (National Instruments) and LabVIEW 2015 software (National Instruments).

pTRIPZ–Prelamin A, pTRIPZ-*LMNB1*, pTRIPZ-*LMNB2*, and pLenti6-EGFP-KASH2 Lentiviral Vectors. The doxycycline-inducible vector pTRIPZ-hDDX5/17 (Addgene) was digested with restriction enzymes *Age*I and *Eco*RI and gel-purified. For the pTRIPZ–Prelamin A vector, a human prelamin A cDNA in pCMV-XL5 vector (#SC101048; Origene) was subcloned into pTRIPZ with Infusion Cloning (Clontech). For the pTRIPZ-*LMNB1*, a human lamin B1 cDNA in pCMB6-XL4 vector (#SC116661; Origene) was amplified with the Titanium Taq PCR kit (Clontech) and sequence-specific primers (forward primer, 5′–GTCAGATCGCACCGGATGGCGACTG–3′; reverse primer, 5′–GTAGCCCCTTGAATTTTACATAATTGCACAGC–3′). For the pTRIPZ-*LMNB2*, a human lamin B2 cDNA in pCMV6-XL4 vector (#SC106163; Origene) was amplified with the Titanium Taq PCR kit (Clontech) and sequence-specific primers (forward primer, 5′–ATGCGTGTGGACCTGGAGAAA–3′; reverse primer, 5′–GTAGCCCCTTGAATTTCACATCACGTAGCAGCCTCTTGA–3′). Each fragment (*LMNB1* and *LMNB2*) was purified with UltraClean15 (Qiagen; Germantown, MD) and subcloned into pTRIPZ vector with Infusion Cloning (Clontech). The products were amplified in XL10-Gold Ultracompetent cells (Agilent; Santa Clara, CA), and plasmids with the correct sequence were isolated with plasmid kits (Qiagen). Packaging of lentivirus and transduction of cells were performed by UCLA's Vector Core. Transduced cells were selected for one week with 1.5 μg/ml puromycin (Gibco) and serially diluted to isolate clones. Doxycycline (Fisher Scientific) was added at the indicated doses to induce expression. The EGFP-KASH2 sequence was amplified from pEGFP-C1-KASH2 (2) as described (3). Briefly, gel-purified fragments were subcloned into the pLenti6/v5-DEST plasmid (ThermoFisher). Packaging of lentivirus and transduction of cells were performed by UCLA's Vector Core. Transduced cells were selected for one week with 2 μg/ml blasticidin (Gibco). Packaging of lentivirus and transduction of cells were performed by UCLA's Vector Core. Transduced cells were subjected to selection for one week with 1.5 μg/ml puromycin or 2 μg/ml blasticidin (Gibco). Doxycycline (Fisher Scientific) was added to induce protein expression.

Supplementary Figures

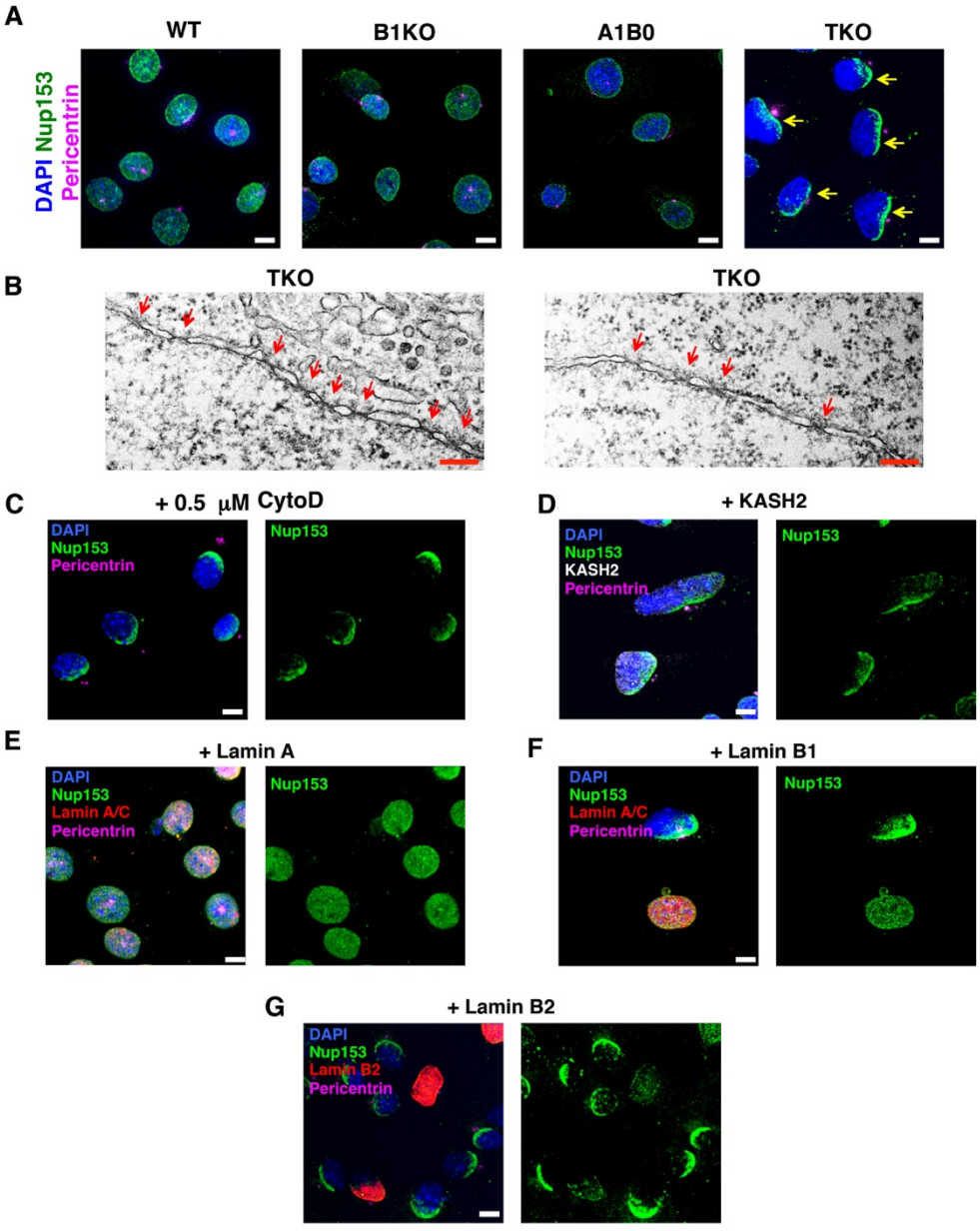

Fig. S1. Abnormal nuclear pore complex (NPC) distribution in TKO MEFs and rescue with individual nuclear lamins. (*A*) Confocal immunofluorescence micrographs showing asymmetric distribution of NPCs (close to the centrosome; *yellow* arrows) in MEFs lacking all nuclear lamins but an even distribution in WT, *Lmna*$^{+/+}$*Lmnb1*$^{-/-}$*Lmnb2*$^{+/+}$ (B1KO), and *Lmna*$^{+/-}$*Lmnb1*$^{-/-}$*Lmnb2*$^{-/-}$ (A1B0) MEFs. MEFs were stained with antibodies against the nuclear pore protein Nup153 (*green*) and the centrosome marker pericentrin (*magenta*). (Scale bars, 10 μm.) (*B*) Electron micrographs showing a high density of NPCs (*red* arrows) in segments of the nuclear envelope in TKO MEFs (Scale bars, 200 nm.) (*C*) Treating TKO MEFs with cytochalasin D made the nuclei rounder but did not rescue nucleoporin distribution. MEFs

were stained with antibodies against the NPC protein Nup153 and pericentrin. (*D*) KASH2-EGFP expression did not rescue nucleoporin distribution in TKO MEFs. MEFs were stained with antibodies against the nuclear pore protein Nup153 and pericentrin. (*E*) Prelamin A expression normalized NPC distribution in TKO MEFs. MEFs were stained with antibodies against lamin A/C (*red*), Nup 153, and pericentrin. (*F*) Lamin B1 expression normalized NPC distribution in TKO MEFs. MEFs were stained with antibodies against lamin B1 (*red*), Nup 153, and pericentrin. (*G*) Lamin B2 expression in TKO MEFs resulted in a change in NPC distribution that matched lamin B2's expression pattern. MEFs were stained with antibodies against lamin B2 (*red*), Nup 153, and pericentrin. In panels *C–E*, Nup153 is in *green*, pericentrin is in *magenta*, and DNA was stained with DAPI (*blue*). (Scale bars in panels *C–G,* 10 μm.)

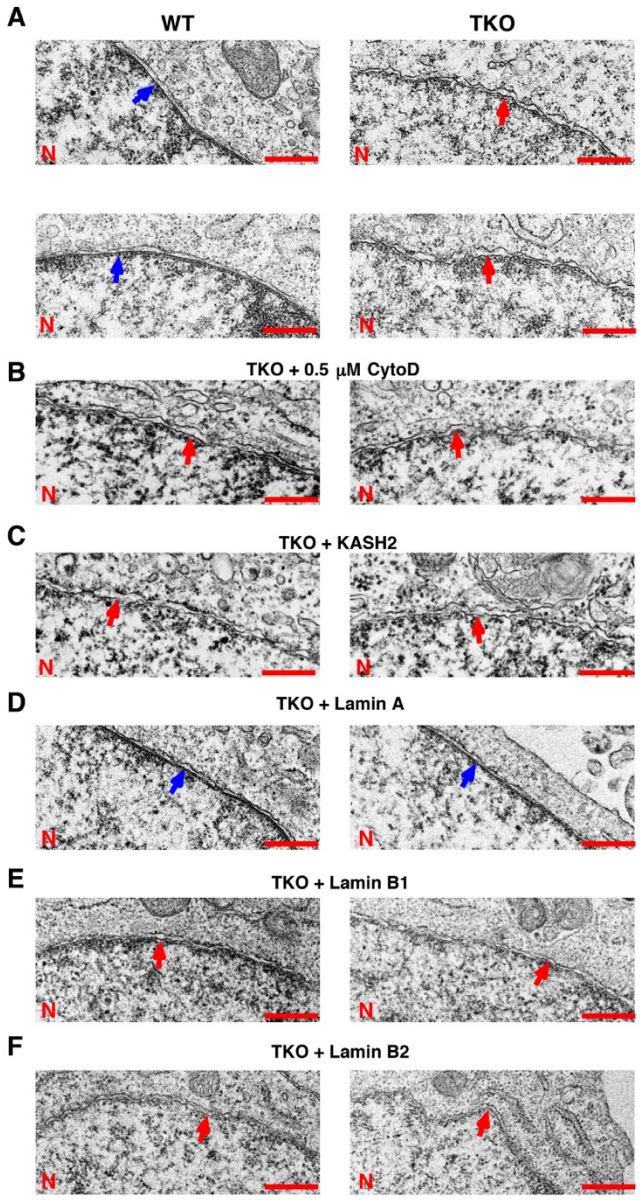

Fig. S2. (*A*) Electron micrographs showing "wavy" inner nuclear membranes in *Lmna*$^{-/-}$*Lmnb1*$^{-/-}$*Lmnb2*$^{-/-}$ (TKO) mouse embryonic fibroblasts (MEFs) (*red* arrows), and relatively straight inner nuclear membranes in wild-type (WT) MEFs (*blue* arrows). (Scale bars, 500 nm.) (*B–F*) Cytochalasin D treatment (*B*) or KASH2-EGFP expression (*C*) did not normalize the wavy inner nuclear membrane phenotype in TKO MEFs. Prelamin A expression (*D*) normalized the wavy inner nuclear membrane phenotype but lamin B1 (*E*) or lamin B2 (*F*) had little or no effect. (Scale bars, 500 nm.)

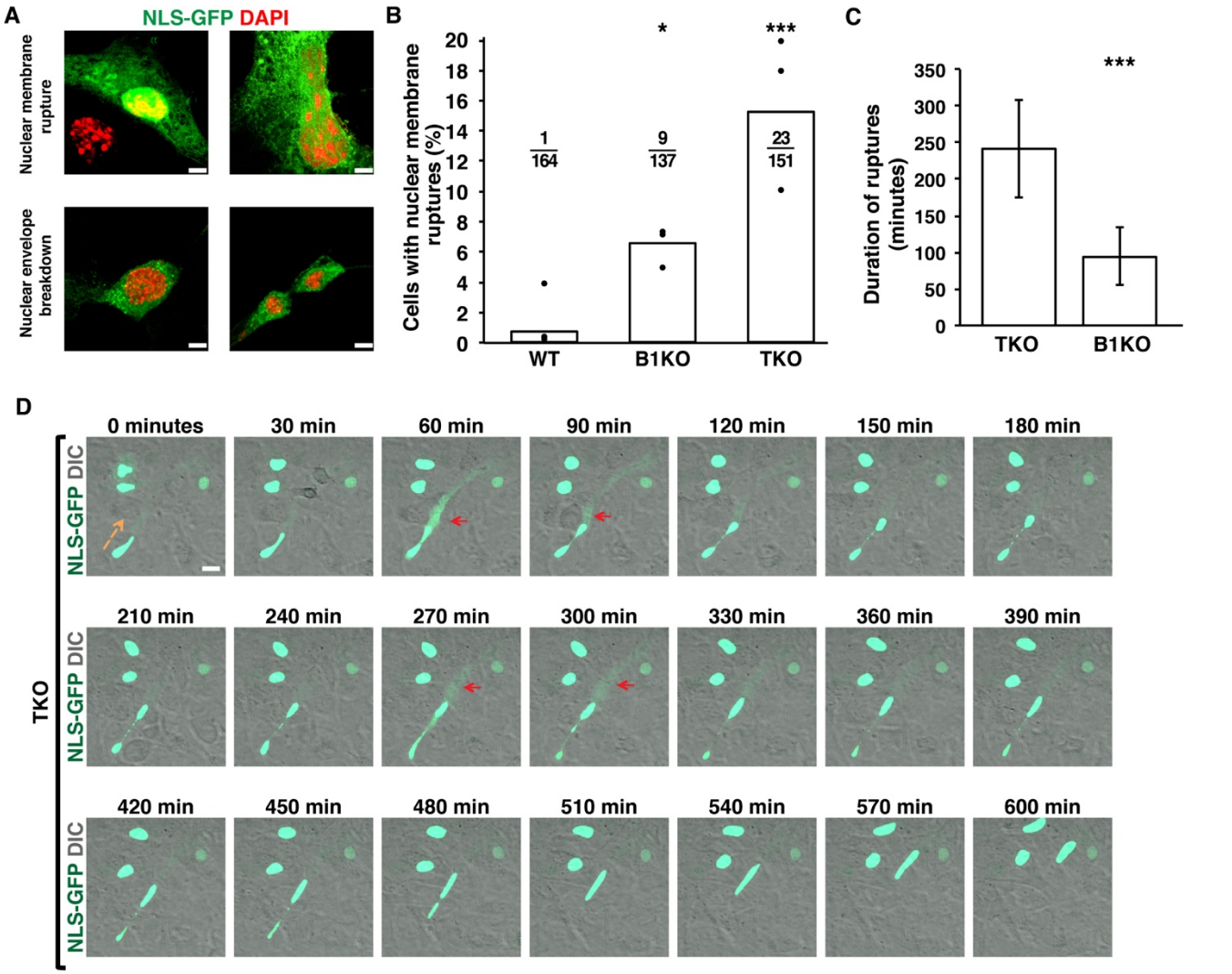

Fig. S3. Nuclear membrane ruptures in *Lmna*$^{+/+}$*Lmnb1*$^{+/+}$*Lmnb2*$^{+/+}$ (wild-type; WT), *Lmna*$^{+/+}$*Lmnb1*$^{-/-}$ *Lmnb2*$^{+/+}$ (lamin B1 knockout; B1KO), and *Lmna*$^{-/-}$*Lmnb1*$^{-/-}$*Lmnb2*$^{-/-}$ (TKO) mouse embryonic fibroblasts (MEFs). (*A*) Confocal micrographs showing TKO MEFs expressing NLS-GFP (*green*) and DNA stained with DAPI (*red*). Nuclear membrane ruptures (*top*) are easily distinguished from mitotic nuclear envelope breakdown (*bottom*) by the DNA staining pattern (*i.e.,* condensed chromatin in mitotic cells), the cytoplasmic shape, and the presence of two nuclei at the end of cell division. (Scale bars, 5 μm.) (*B*) Bar graph showing percentages of MEFs with nuclear membrane ruptures during 20 h of imaging. Nuclear membrane ruptures were more frequent in B1KO and TKO MEFs than in WT MEFs. *$P < 0.05$, ***$P < 0.0005$ by x^2 test. (*C*) Bar graph showing the average duration of nuclear membrane ruptures in TKO and B1KO MEFs (average of 10 nuclear membrane ruptures per group). ***$P < 0.0001$ by Student's *t* test. (*D*) Image sequence showing multiple nuclear membrane ruptures (*red* arrows) in a migrating TKO MEF. NLS-GFP is in *green* and DIC is in *gray*. (Scale bar, 20 μm.)

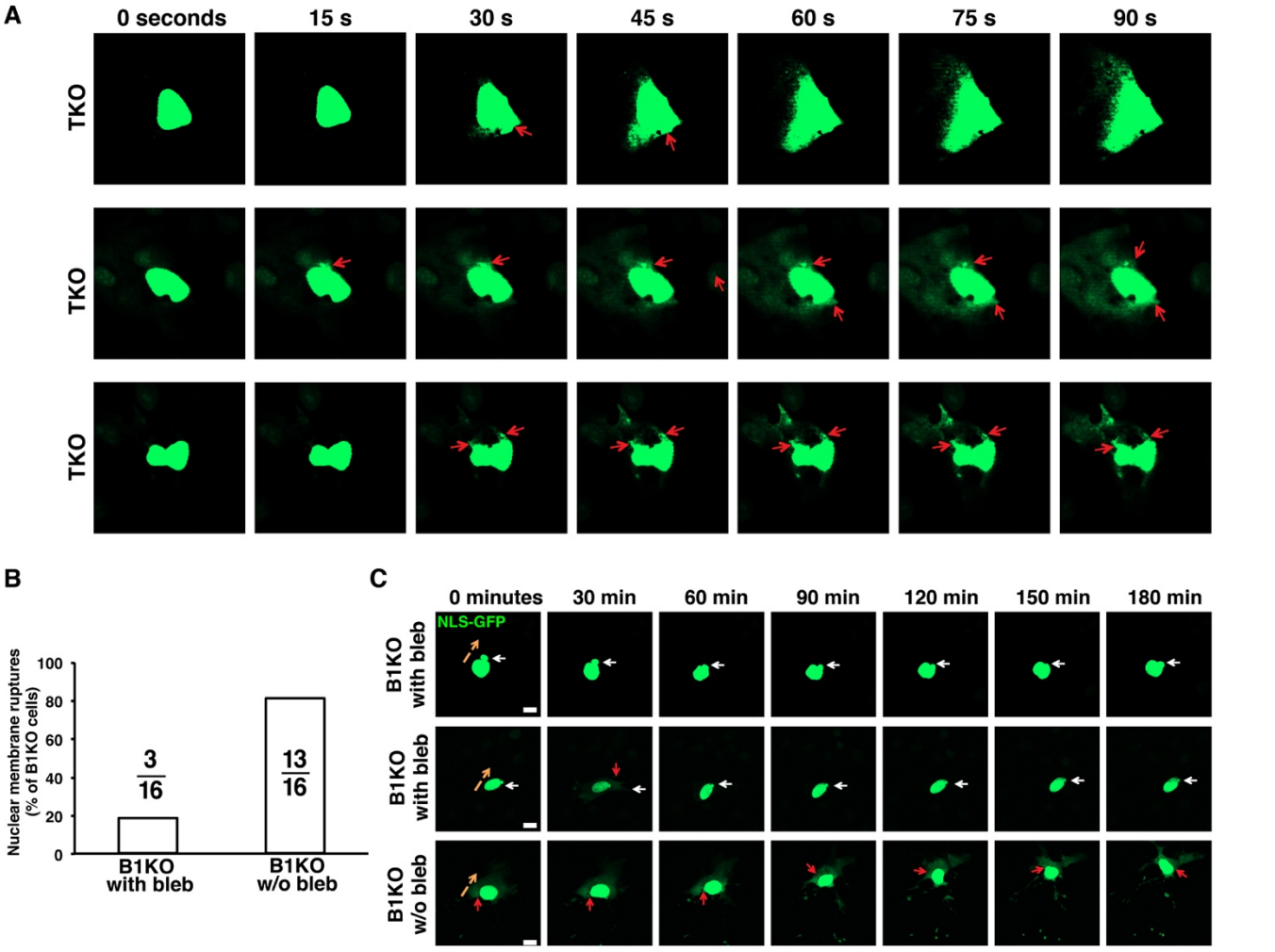

Fig. S4. Nuclear blebs are not a prerequisite for nuclear membrane ruptures. (*A*) Image sequences of three separate nuclear membrane rupture events in TKO MEFs (*top*, *middle*, *bottom*), where nuclear membrane ruptures occur in cells lacking a nuclear bleb. *Red* arrows show where nuclear membrane ruptures first appear in each cell. (*B*) Bar graph showing percentages of nuclear membrane ruptures in B1KO MEFs in cells with nuclear blebs *vs*. cells without nuclear blebs during 20 h of imaging. Only three of 33 nuclear membrane rupture events occurred in nuclei with a nuclear bleb. (*C*) Three image sequences of B1KO MEFs: (*top*) a B1KO nucleus with a nuclear bleb but no nuclear membrane ruptures; (*middle*) a B1KO nucleus with a nuclear bleb and one rupture event (*red arrow*); (*bottom*) a B1KO nucleus without a nuclear bleb but with a nuclear membrane rupture (*red arrow*). *Orange* arrows indicate direction of nuclear translocation. (Scale bars, 20 μm.)

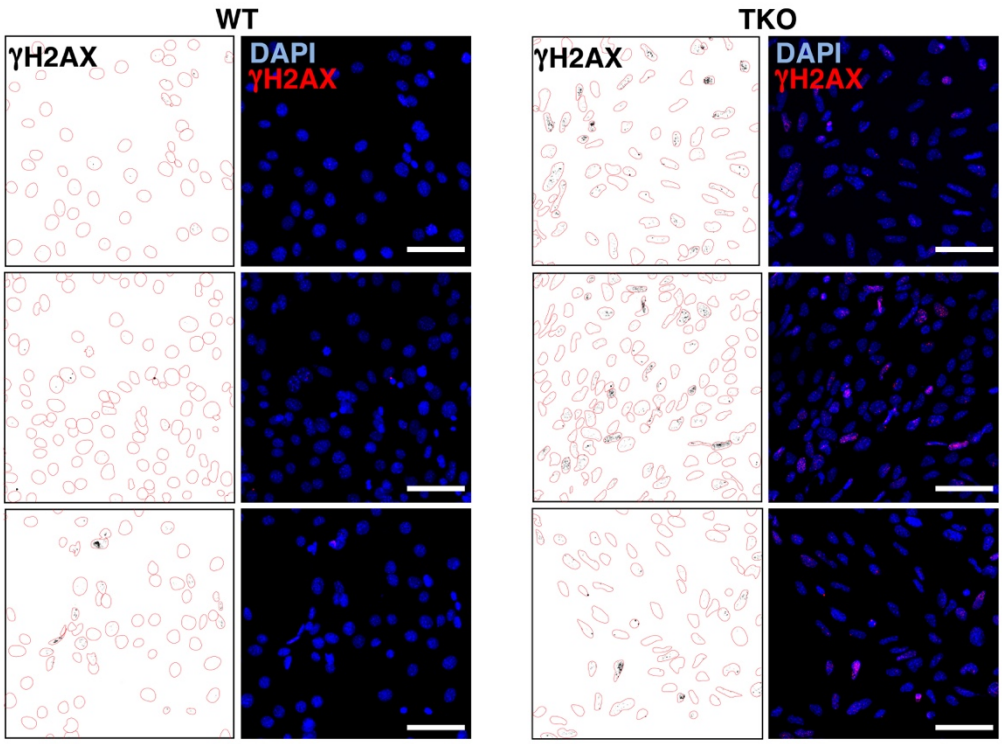

Fig. S5. Confocal immunofluorescence micrographs of wild-type (WT) and *Lmna*$^{-/-}$*Lmnb1*$^{-/-}$*Lmnb2*$^{-/-}$ (TKO) MEFs, revealing larger numbers of γ-H2AX foci in TKO MEFs than in WT MEFs. In the fluorescence microscopy images, γ-H2AX foci are colored *red*, and the nuclei are stained with DAPI (blue). To better visualize the γ-H2AX foci, drawings of the microscopy images were generated. In the drawings, the perimeter of each nucleus is outlined in *red* and γ-H2AX foci are shown in *black*. (Scale bars, 50 μm.)

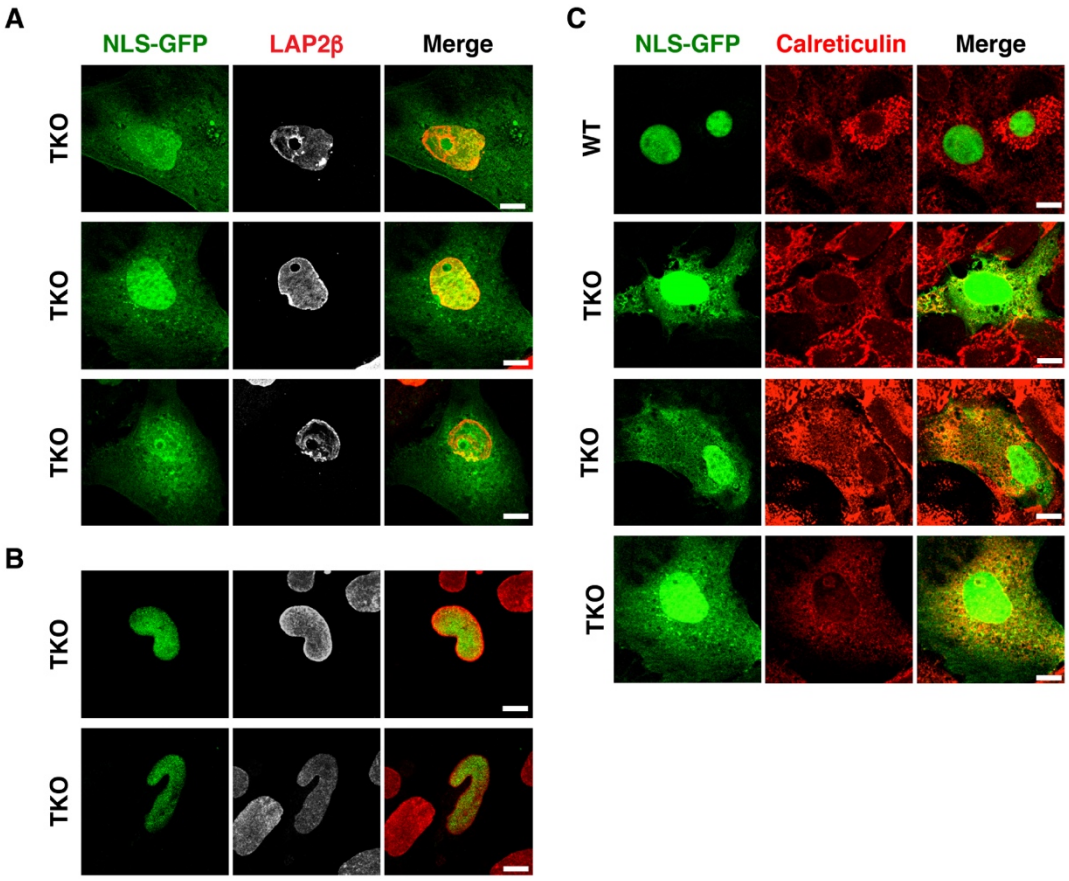

Fig. S6. Abnormal nuclear morphology in *Lmna*$^{-/-}$*Lmnb1*$^{-/-}$*Lmnb2*$^{-/-}$ (TKO) mouse embryonic fibroblasts (MEFs). (*A*) Confocal immunofluorescence micrographs showing an abnormal distribution of LAP2β (an inner nuclear membrane marker; *red*) in TKO MEFs with nuclear membrane ruptures, where NLS-GFP escapes into the cytoplasm. (*B*) Confocal immunofluorescence micrographs showing LAP2β is uniformly distributed in TKO MEFs without nuclear membrane ruptures. Note the abnormal nuclear shape. (*C*) Confocal immunofluorescence micrographs of WT and TKO MEFs that have been stained with an antibody against calreticulin (*red*), a resident protein of the endoplasmic reticulum. NLS-GFP is located exclusively in the nucleus of WT MEFs (*top*), with negligible colocalization with calreticulin. In TKO MEFs, the degree of colocalization between NLS-GFP and calreticulin was variable. (Scale bars in *A*–*C*, 10 μm.)

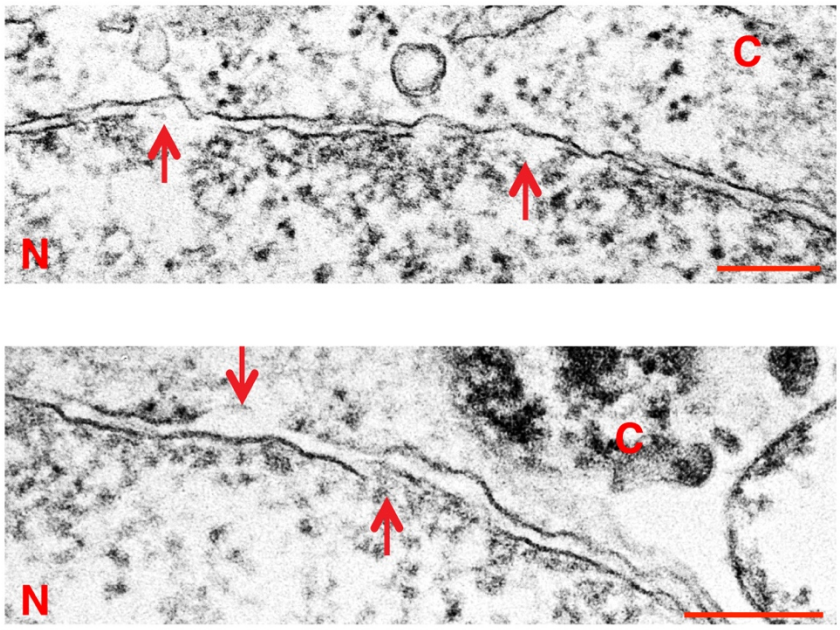

Fig. S7. Electron micrographs of adherent TKO MEFs showing examples of discrete inner and outer nuclear membrane discontinuities (*red* arrows). (Scale bars, 200 nm.) N, nucleus; C, cytoplasm.

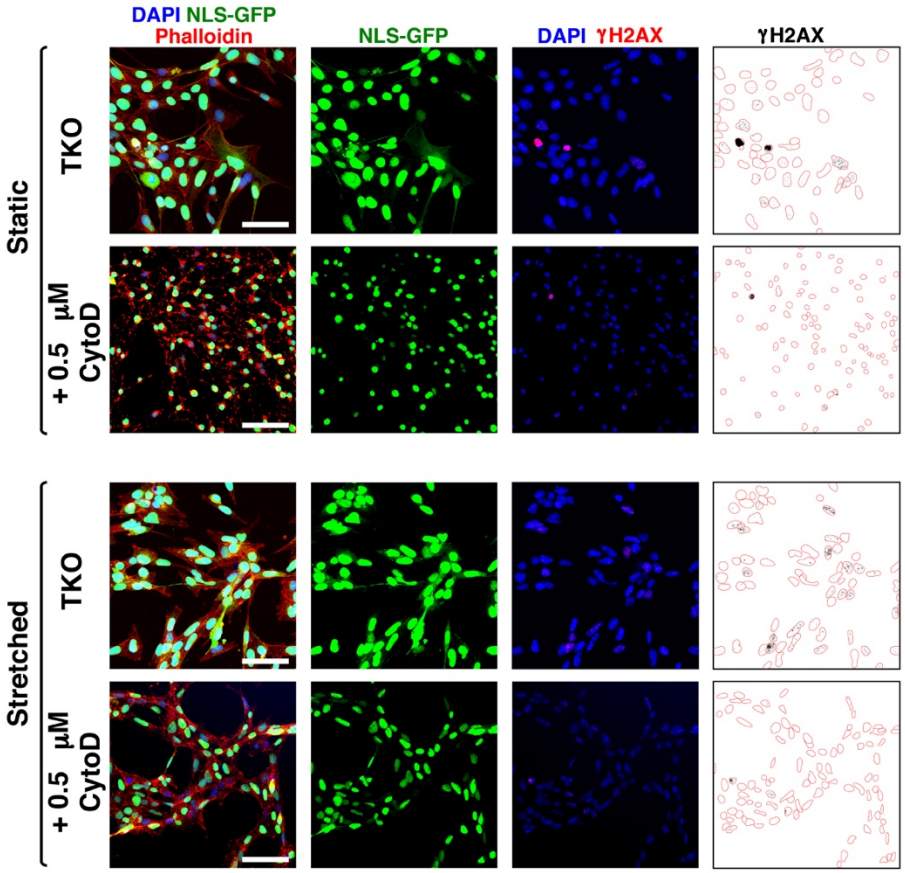

Fig. S8. Confocal immunofluorescence micrographs of TKO MEFs under static conditions (*top*) and with mechanical stretching (*bottom*). Actin depolymerization in TKO MEFs with cytochalasin D results in rounder nuclei, fewer nuclear membrane ruptures [as judged by the escape of NLS-GFP into the cytoplasm], and reduced numbers of γ-H2AX foci in TKO MEFs, both under static and stretched conditions. In the far right panel, the nuclei of TKO MEFs stained with an antibody against γ-H2AX are outlined in *red* and γ-H2AX foci are colored in *black*. The drawings reveal fewer γ-H2AX foci in cells treated with cytochalasin D, both under static and stretched conditions. (Scale bars, 50 μm.)

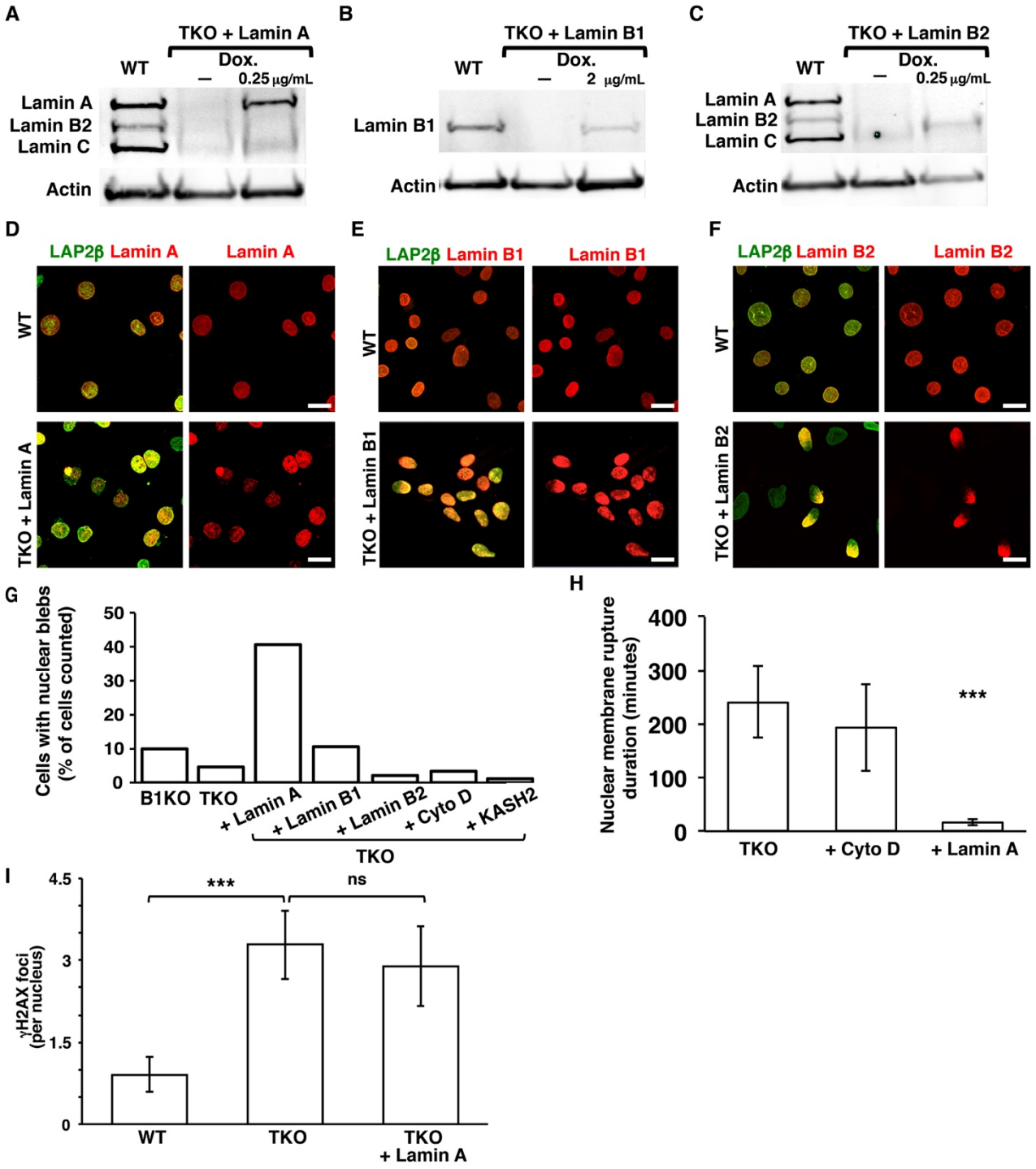

Fig. S9. (*A–C*) Western blot studies of TKO MEFs after introducing expression vectors for prelamin A (pTRIPZ–hu-prelamin A), lamin B1 (pTRIPZ-*LMNB1*), or lamin B2 (pTRIPZ-*LMNB2*) and then inducing expression with doxycycline (Dox.). Lamin expression was compared to wild-type (WT) MEFs. Actin was used as a loading control. (*D*) Immunofluorescence micrographs showing a homogeneous distribution of lamin A in WT MEFs and an uneven ("honeycomb") distribution of lamin A in TKO MEFs that express lamin A (*i.e.*, after being transduced with pTRIPZ–hu-prelamin A). LAP2β is in *green* and lamin A is in

red. (*E*) Immunofluorescence micrographs showing lamin B1 distribution in WT MEFs, and in TKO MEFs that express lamin B1 (*i.e.*, after being transduced with pTRIPZ–*LMNB1*). LAP2β is in *green* and lamin B1 is in *red*. (*F*) Immunofluorescence micrographs showing an even distribution of lamin B2 in WT MEFs and an asymmetric distribution of lamin B2 in TKO MEFs expressing lamin B2. LAP2β is in *green* and lamin B2 is in *red*. (Scale bars in *D–F*, 20 μm.). (*G*) Bar graph showing the percentage of cells with nuclear blebs in TKO MEFs with lamin A expression, lamin B1 expression, lamin B2 expression, cytochalasin D treatment, and KASH2 expression. B1KO MEFs are include as a control. (*H*) Bar graph shows the average duration of nuclear membrane ruptures in TKO MEFs, TKO MEFs treated with 0.5 μM cytochalasin D, and TKO MEFs expressing lamin A. Nuclear membrane rupture duration was shorter in TKO MEFs expressing lamin A. ***$P < 0.0001$ by Student's *t* test. (*I*) Bar graph showing that expression of lamin A does not reduce γ-H2AX foci in TKO MEFs. The results were analyzed as described in *G*. ***$P < 0.0005$; nonsignificant (ns, $P > 0.05$ by Student's *t* test).

Supplementary Tables S1–S2

Table S1

Gene	Species	Sequences (5′–3′)
Lamin A	Mouse	ggttgaggacaatgaggatga tgagcgcaggttgtactcag
Lamin B1	Mouse	caactgacctcatctggaagaac tgaagactgtgcttctctgagc
Lamin B2	Mouse	aggtgcaggctgagctagag tgattccagatccttcactcg
Lamin C	Mouse	cctatcgaaagctgctggag cctgagactgggatgagtgg
Cyclophilin A	Mouse	tgagcactggagagaaagga ccattatggcgtgtaaagtca

Table S2

Antigen	Antibody	Species	Company	WB	ICC
Lap2β [27]	Monoclonal	Mouse	BD Transduction Lab		1:500
Lamin B1 [M-20]	Polyclonal	Goat	Santa Cruz Biotech.	1:2000	1:500
Pericentrin	Polyclonal	Rabbit	Abcam		1:1000
Lamin A/C	Polyclonal	Goat	Santa Cruz Biotech.		1:500
Lamin A	Monoclonal	Mouse	Santa Cruz. Biotech	1:2000	
Lamin B2	Monoclonal	Rabbit	Abcam		1:1000
Lamin B2	Monoclonal	Mouse	Invitrogen		1:50
Lamin B2	Polyclonal	Rabbit	Proteintech	1:300	
Actin	Polyclonal	Goat	Santa Cruz Biotech.	1:5000	
Nup 153	Monoclonal	Mouse	Abcam		1:250
TurboGFP	Polyclonal	Rabbit	Thermo Fisher Scientific		1:1000
eGFP	Polyclonal	Rabbit	Invitrogen		1:1000
Phalloidin-546			Invitrogen		1:2000
γ-H2AX	Monoclonal	Rabbit	EMD Millipore		1:1000

Captions for Movies S1–S15

Movies S1 and S2. TKO MEFs exhibit transient nuclear membrane ruptures. TKO MEFs (Movie S2) expressing NLS-GFP (*green*) were imaged over 240 min and exhibit transient nuclear membrane ruptures (flooding of NLS-GFP into the cytoplasm). WT MEFs (Movie S1) imaged over 240 min do not exhibit nuclear membrane ruptures. DIC is in *gray*.

Movie S3. A TKO MEF exhibits nuclear membrane rupture and nuclear fragmentation. TKO MEFs expressing NLS-GFP (*green*) were plated at high density and imaged over 500 min. A TKO MEF exhibits a nuclear membrane rupture and subsequent nuclear fragmentation. DIC is in *gray*.

Movies S4–6. Nuclear membrane ruptures do not occur through nuclear blebs/herniations in TKO MEFs. TKO MEFs expressing NLS-GFP (*green*) were imaged over 150 sec at 15-sec intervals. Each movie (S6, S7, S8) documents a distinct example of a nuclear membrane rupture in the absence of a nuclear bleb. DIC is in *gray*.

Movies S7–S9. B1KO MEFs occasionally exhibit nuclear membrane ruptures but they do not always coincide with the presence of a nuclear bleb. B1KO MEFs expressing NLS-GFP (*green*) were imaged over 180 min. A B1KO MEF with a nuclear bleb does not have a nuclear membrane rupture (Movie S3). An occasional B1KO MEF with a nuclear bleb does exhibit a nuclear membrane rupture (Movie S4). More often, B1KO MEFs without a nuclear bleb have nuclear membrane ruptures (Movie S5). DIC is in *gray*.

Movies S10 and S11. TKO MEFs with nuclear membrane ruptures leading to cell death. TKO MEFs expressing NLS-GFP (*green*) were imaged over time. (Movie S10) NLS-GFP persists in the cytoplasm. Time interval, 890 min. (Movie S11) In Movie S11, NLS-GFP in the cytoplasm was as intense as in the nucleoplasm. Time interval: 1120 min.

Movie S12. Cytochalasin D prevents nuclear membrane ruptures in TKO MEFs. TKO MEFs expressing NLS-GFP (*green*) were treated with 0.5 mM of cytochalasin D for 1 h and then imaged for 240 min. In the presence of cytochalasin D, the nucleus is rounder and does not exhibit nuclear membrane ruptures. DIC is in *gray*. Time interval: 240 min.

Movies S13–15. Expression of lamin A, lamin B1, or lamin B2 in TKO MEFs does not prevent nuclear membrane ruptures. TKO MEFs expressing NLS-GFP (*green*) were transduced with an inducible expression vector for lamin B1 (Movie S13), lamin B2 (Movie S14), or lamin A (Movie S15). Each movie captures a nuclear membrane rupture. DIC is in *gray*. Time interval: 240 min.

References for SI

1. Rowat AC, Jaalouk DE, Zwerger M, Ung WL, Eydeinant IA, Olins DE, Olins AL, Herrmann H, Weltz DA, Lammerding J (2013) Nuclear envelope composition determines the ability of neutrophil-type cells to passage through micron-scale constrictions. *J Biol Chem* **288**:8610–8618.
2. Stewart-Hutchinson PJ, Hale CM, Wirtz D, Hodzic D (2008) Structural requirements for the assembly of LINC complexes and their function in cellular mechanical stiffness. *Exp Cell Res* **314**:1892–1905.
3. Kim P*, et al.* Disrupting the LINC complex in smooth muscle cells ameliorates aortic disease in a mouse model of Hutchinson-Gilford progeria syndrome. *Sci. Transl. Med. (in press)*.